

# Emerging Entities and New Diagnostic Markers for Head and Neck Soft Tissue and Bone Tumors

Alessandro Franchi, MD,\* Lester D.R. Thompson, MD,†

Juan C. Hernandez-Prera, MD,‡ Abbas Agaimy, MD,§

Michelle D. Williams, MD,|| Lauge H. Mikkelsen, MD,¶ Justin A. Bishop, MD,#

Stefan M. Willems, MD,\*\*†† Henrik Hellquist, MD,‡‡ and Alfio Ferlito, MD§§

**Abstract:** Bone and soft tissue tumors of the head and neck are relatively uncommon tumors that often represent a diagnostic challenge because of the wide range of entities that must be considered in the differential diagnosis. Over the past few years, classification of bone and soft tissue tumors has evolved primarily because of substantial contributions from molecular genetics, with the identification of new markers that are increasingly used to complement histopathologic findings in the routine diagnostic workup. This review focuses on the recently described mesenchymal tumors that preferentially involve the head and neck region, with a focus on the most relevant novel immunohistochemical and molecular findings, including gene fusions and mutations, that can help in the diagnosis and in the assessment of clinical behavior.

**Key Words:** head and neck, bone tumors, soft tissue tumors, diagnostic markers, immunohistochemistry, molecular genetics

(*Adv Anat Pathol* 2021;00:000–000)

**B**one and soft tissue tumors of the head and neck are relatively uncommon, with malignant neoplasms accounting for ~1% of all head and neck malignancies, but representing 5% to 10% of all soft tissue sarcomas and showing a relatively higher incidence in pediatric patients.<sup>1–4</sup> The involved soft tissue sites include the somatic soft tissues (mainly the neck, scalp, and the face) and mucosal or glandular sites (sinonasal tract and skull base, tongue and oral cavity, parotid gland), whereas bone

tumors affect the gnathic bones, paranasal sinuses, and laryngeal cartilages.

Although in general it is thought that the natural history of head and neck sarcomas parallels that of non-head and neck sites, the complex anatomy of this region represents a limit to wide surgical resections and may explain worse local disease control.

Currently, surgery is considered the main treatment in low-grade sarcomas, whereas high-grade sarcomas can be treated with neoadjuvant chemotherapy followed by surgery and radiotherapy.<sup>4</sup>

A wide variety of sarcomas arise in the soft tissues of the head and neck, with a relative frequency that depends on the age and anatomic location. In adults, adipocytic tumors and malignant peripheral nerve sheath tumors predominate, whereas in pediatric patients, rhabdomyosarcoma (RMS) is the most frequent histologic type. Notably, some of the mesenchymal tumors arising in the head and neck are distinctive to these sites or occur preferentially in these regions, such as biphenotypic sinonasal sarcoma or some RMS variants. An important aspect that must be considered in the diagnostic workup of mesenchymal lesions of the head and neck with spindle or with spindle/pleomorphic morphology in adult patients is that spindle cell (sarcomatoid) squamous cell carcinoma and melanoma are more common than any sarcoma type, and should therefore be at the top of the list of differential diagnoses. Still, head and neck soft tissue tumors often represent a diagnostic challenge because of the wide range of entities that must be considered in the differential diagnosis, compounded by small biopsies that often have crush artifacts.

Over the past few years, the classification of bone and soft tissue tumors has evolved primarily due to a better understanding of their biology, with substantial contributions from molecular genetics and immunohistochemical findings. Thus, immunohistochemical and molecular markers are increasingly used to complement histopathologic findings in the diagnosis of head and neck soft tissue tumors, but also in some instances to refine prognostication or to support targeted therapeutic approaches. Moreover, the advancement in molecular techniques now allows for interrogation of small tissue samples, including aspirate material for DNA and RNA alterations.<sup>5</sup> Compared with traditional single-gene evaluation, next-generation sequencing platforms can simultaneously evaluate large panels of markers. Further, molecular panels tailored specifically for sarcomas are utilized clinically.

This review discusses the recently described soft tissue and bone tumors that preferentially involve the head and neck region, with a focus on the most relevant novel immunohistochemical and molecular findings, including gene fusions and mutations, that can help in the diagnostic workup and in the assessment of clinical behavior.

From the \*Department of Translational Research and of New Technologies in Medicine and Surgery University of Pisa, Pisa; §International Head and Neck Scientific Group, Padua, Italy; †Department of Pathology, Southern California Permanente Medical Group, Woodland Hills Medical Center, Woodland Hills, CA; ‡Department of Pathology, Moffitt Cancer Center, Tampa, FL; §Institute of Pathology, University Hospital, Friedrich-Alexander University Erlangen-Nürnberg, Erlangen, Germany; ||Department of Pathology, University of Texas MD Anderson Cancer Center, Houston; #Department of Pathology, University of Texas Southwestern Medical Center, Dallas, TX; ¶Department of Pathology, Eye Pathology Section, Rigshospitalet, Copenhagen University Hospital, Copenhagen, Denmark; \*\*Department of Pathology, University Medical Center Utrecht, Utrecht; ††Department of Pathology and Medical Biology, University Medical Center Groningen, Groningen, The Netherlands; and ‡‡Epigenetics and Human Disease Laboratory, Department of Biomedical Sciences and Medicine, University of Algarve, Faro, Portugal.

This article was written by members and invitees of the International Head and Neck Scientific Group ([www.IHNSG.com](http://www.IHNSG.com)).

The authors have no funding or conflicts of interest to disclose.

Reprints: Alessandro Franchi, MD, Department of Translational Research and of New Technologies in Medicine and Surgery, University of Pisa, Via Paradisa 2, Pisa 56124, Italy (e-mail: [alessandro.franchi@unipi.it](mailto:alessandro.franchi@unipi.it)).

All figures can be viewed online in color at [www.anatomicpathology.com](http://www.anatomicpathology.com). Copyright © 2021 Wolters Kluwer Health, Inc. All rights reserved.

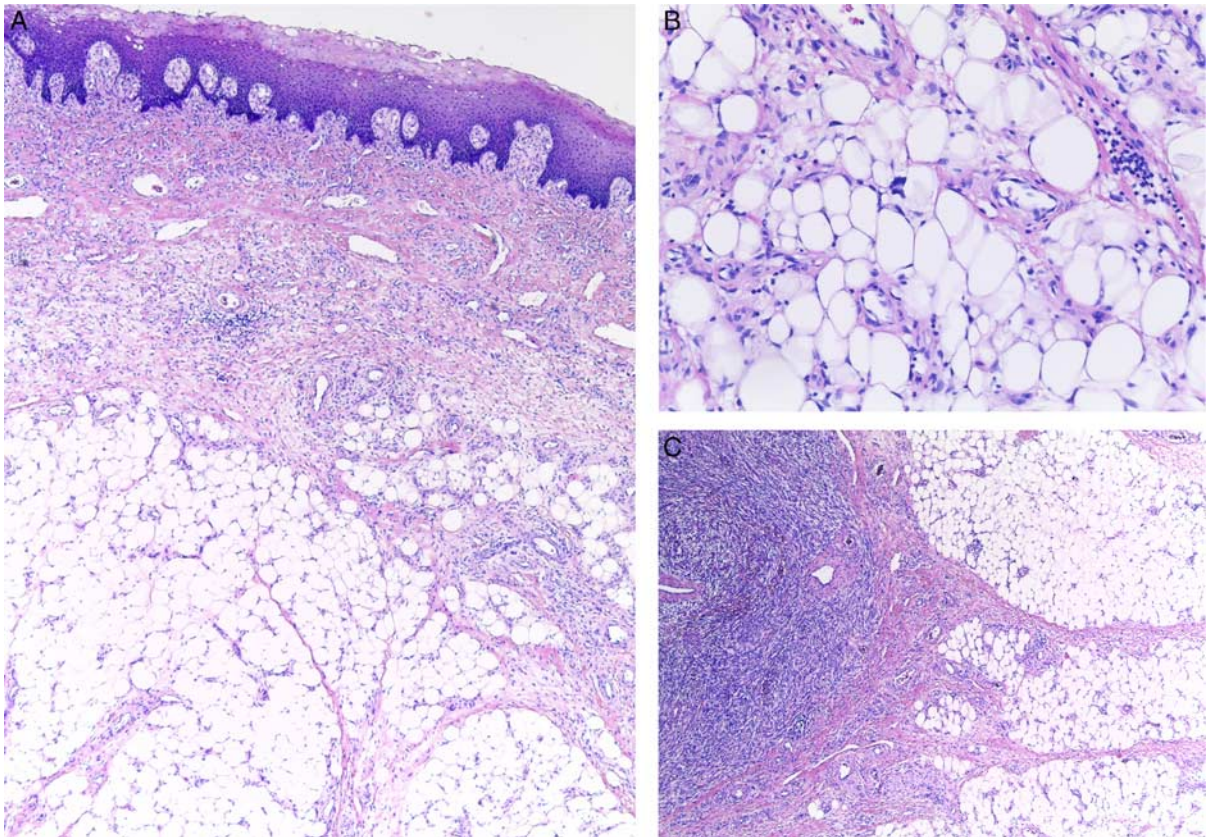


**FIGURE 1.** Polypoid lesion of the hypopharynx in a 62-year-old man. A subepithelial fatty tumor is present (A), which at higher power consists of adipocytes of variable size and atypical cells, including multinucleated elements (B). A second component of spindle cells, well demarcated from the fatty component, is present in the center of the tumor (C). On the basis of amplification of *MDM2* detected by FISH analysis, the final diagnosis was dedifferentiated liposarcoma.

### ADIPOCYTIC TUMORS

A variety of adipocytic tumors arise in the head and neck region, but liposarcomas are rare in these sites, with well-differentiated/dedifferentiated liposarcomas (WDL/DL) mainly involving the larynx, hypopharynx, oral cavity, and the neck<sup>6,7</sup> (Fig. 1).

It is recognized that WDL/DL often represent a diagnostic challenge, being easily confused with benign adipocytic tumors or nonadipocytic soft tissue proliferations, including nodular fasciitis, mammary-type myofibroblastoma, low-grade myofibroblastic sarcoma, and undifferentiated pleomorphic sarcoma.<sup>6</sup> Nevertheless, an accurate diagnosis of WDL/DL informs the prognosis of head and neck tumors, which is worse than in other sites.<sup>8</sup> In selected cases, identification of *MDM2* and/or *CDK4* expression by immunohistochemistry or amplification by fluorescence in situ hybridization (FISH) or other molecular techniques may be necessary to support the diagnosis of WDL/DL.<sup>9</sup> However, a possible diagnostic pitfall is represented by lipomas with degenerative changes that may mimic ALT for the presence of increased stromal cellularity and of multivacuolated histiocytes that superficially resemble lipoblasts.<sup>10</sup> As *MDM2* immunohistochemical expression may occur in histiocytes, confirmation with search for *MDM2* amplification by FISH or other molecular methods may be necessary to avoid overdiagnosis.<sup>10</sup> Further, *STAT6* immunoreactivity is reported in rare examples of DL.<sup>7,11,12</sup>

This marker is used in solitary fibrous tumors, a spindle cell neoplasm also affecting head and neck sites, that may occasionally contain mature adipocytes, thus closely resembling WDL/DL. However, nuclear positivity for *MDM2* by immunohistochemistry or *MDM2* amplification will help support the diagnosis of DL.

Atypical spindle cell/pleomorphic lipomatous tumor is a recently described adipocytic neoplasm included in the fifth edition of the World Health Organization (WHO) Classification of Soft Tissue and Bone Tumours.<sup>13</sup> It only rarely arises in the head and neck, affecting the soft tissues of the neck and face, and less frequently the larynx/hypopharynx.<sup>14,15</sup> Most of these tumors had been previously included in the group of “spindle cell liposarcoma,” as they are composed of an admixture of atypical spindle cells, adipocytes, lipoblasts, and may contain hyperchromatic and bizarre pleomorphic cells (Fig. 2). Myxoid or collagenous matrix, often with characteristic brightly eosinophilic “ropy” collagen fibers, is present in the intercellular space. They are currently considered as benign neoplasms, with low tendency for local recurrence and no risk for dedifferentiation. Thus, they have to be distinguished from WDL that show a risk for destructive recurrence and/or progression to DL. Tumor cells in atypical spindle cell lipomatous tumors are variably positive for *CD34*, *S100* protein, and *desmin*, whereas *MDM2* and *CDK4* are usually negative or weakly positive in few cells. In addition, loss of nuclear *RB1* expression is observed in 50% to 70% of

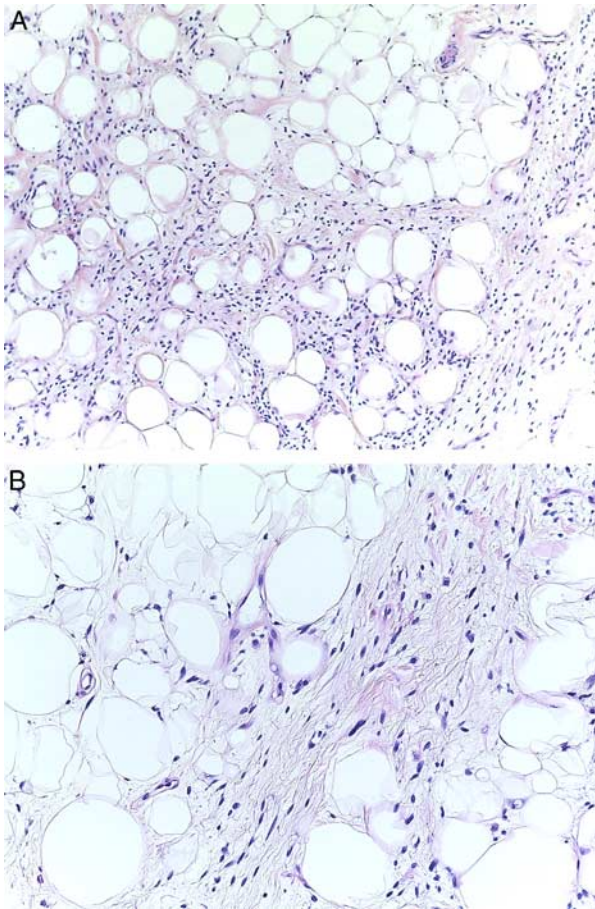


**FIGURE 2.** Atypical spindle cell lipomatous presenting an adipocytic component with marked variation in adipocyte size and shape admixed with a spindle cell component in a myxoid background with delicate collagen fibers (A). At higher power lipoblasts can be detected in the adipocytic component together with scattered atypical spindle cells with hyperchromatic nuclei (B). Please see this image in color online.

atypical spindle cell lipomatous tumors, whereas *MDM2* amplification is absent. Spindle cell lipoma is usually circumscribed, may show rare lipoblasts, but shows uniform and elongated nuclei. Nuclear RB1 protein loss can also be seen.<sup>16</sup>

### SPINDLE CELL TUMORS

Ectomesenchymal chondromyxoid tumor (ECT) is an increasingly recognized but still a debated entity of uncertain histogenesis, which is thought to derive from undifferentiated ectomesenchymal cells.<sup>17</sup> It occurs preferentially in the anterior dorsal tongue, although it has rarely been reported at other intraoral sites and in the mandible.<sup>18</sup>

Histologically, ECT is well circumscribed and unencapsulated, and shows a multilobulated growth pattern, with thin fibrous septa separating a relatively uniform population of bland spindle cells arranged in reticular and globoid patterns within an abundant myxoid matrix (Fig. 3). Focal atypia, binucleation, pseudonuclear inclusions, and necrosis may occasionally be present, while mitotic activity is usually sparse. The immunohistochemical profile of this tumor includes positivity for glial fibrillary acid protein,

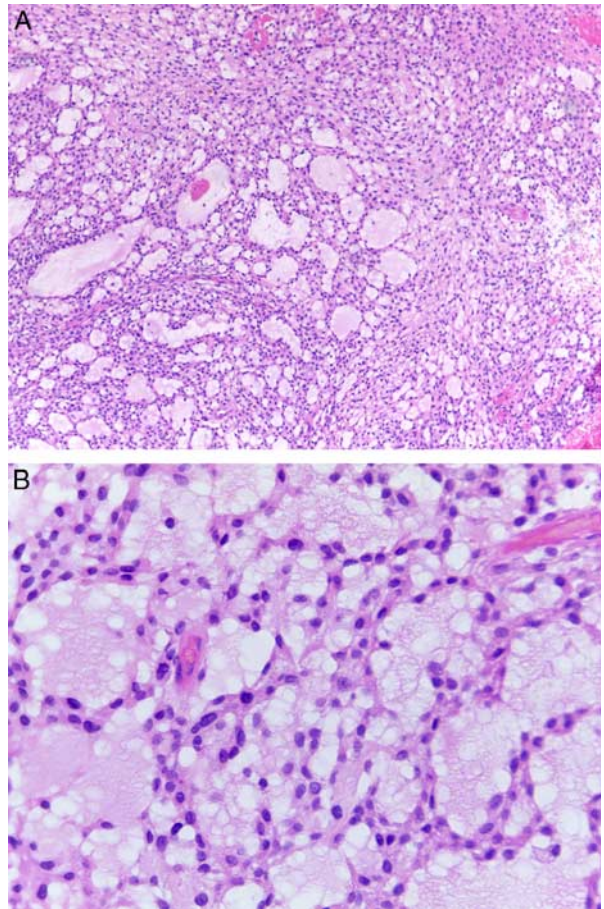


**FIGURE 3.** Ectomesenchymal chondromyxoid tumor of the tongue presents with a uniform population of bland spindle and stellate cells arranged in reticular and microcystic patterns (A). Tumor cells are arranged within abundant myxoid matrix (B). Please see this image in color online.

S100 protein, keratin, actins, and desmin.<sup>17</sup> With these histopathologic and immunohistochemical features, ECT has been hypothesized to be akin to soft tissue myoepitheliomas, as the involved sites generally contain no or few mucoserous salivary-type glands. Table 1 compares the immunohistochemical and molecular features of ECT and soft tissue myoepitheliomas. Recently, Dickson et al<sup>19</sup> identified the *RREB1-MRTFB* (previously known as *MKL2*) fusion in 90% of their series of ECT. The same gene fusion has been identified in a histologically identical mandible tumor,<sup>18</sup> in a tumor of the oropharynx,<sup>20</sup> and in 2 mesenchymal tumors arising in the mediastinum.<sup>21</sup> The tumor of the oropharynx showed no involvement of the tongue and was interpreted as related to biphenotypic sinonasal sarcoma, as it showed fascicles of spindle cells immunopositive for S100 protein, smooth muscle actin (SMA), desmin, and myogenin. The mediastinal tumors showed only partially similar histologic and immunohistochemical features to classic ECT<sup>21</sup> but may be considered part of the spectrum of these tumors. Finally, 1 case in the series of Dickson et al<sup>19</sup> and 3 of 11 cases (27%) reported by Argyris et al<sup>22</sup> showed *EWSR1* gene rearrangement. This may support a relationship with soft tissue myoepitheliomas that often present *EWSR1* gene

**TABLE 1.** Comparison of Immunohistochemical and Molecular Features of Ectomesenchymal Chondromyxoid Tumor and Soft Tissue Myoepithelioma

Marker	Ectomesenchymal Chondromyxoid Tumor	Myoepithelioma
Cytokeratin	Positive, 40%*	Positive, 80%
EMA	Positive, 10%	Positive, 70%
S100	Positive, 80%	Positive, 90%
SOX10	Positive, 50%	Positive, 80%
Calponin	Positive, 10%	Positive, 90%
CD56	Positive, 80%	Not tested
CD57	Positive, 75%	Not tested
Synaptophysin	Positive, 70%	Not tested
Smooth muscle actin	Positive, 50%	Positive, 40%
Desmin	Positive, 15%	Positive, 15%
GFAP	Positive, 90%	Positive, 50%
p63	Positive, 40%	Positive, 25%
Myogenin	Negative	Negative
Cyclin D1	Positive	Not tested
Gene fusions	<i>RREB1-MKL2</i> , EWSR1 rearrangement ≅ in 20%	<i>EWSR1</i> gene rearrangement with <i>POU5F1</i> , <i>PBX1</i> , <i>ZNF444</i> , <i>KLF17</i> , <i>ATF1</i> , <i>PBX3</i>

\*Percentage of positive cases.

EMA indicates epithelial membrane antigen; GFAP, glial fibrillary acidic protein.

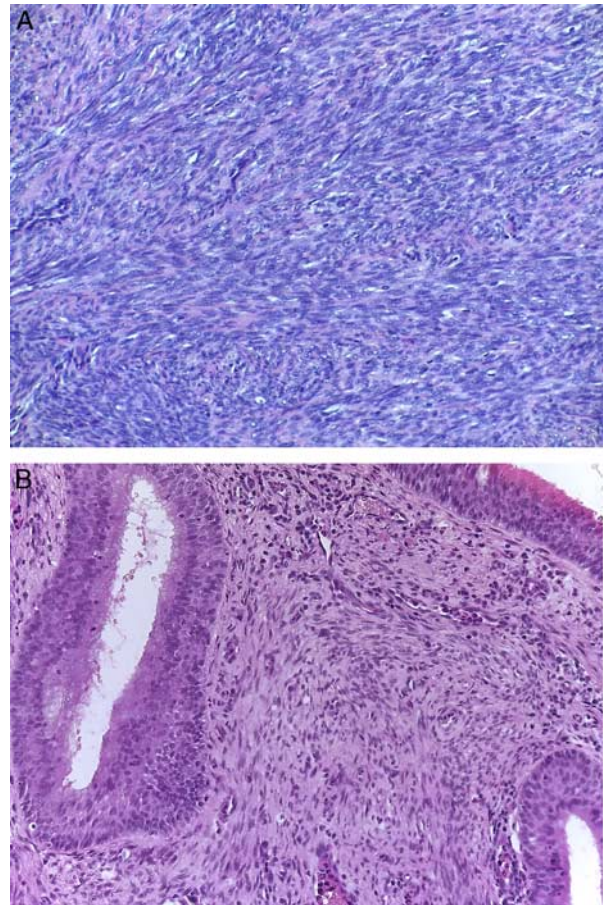


**FIGURE 4.** Biphenotypic sinonasal sarcoma. Neoplastic spindle cells are arranged in fascicles with a herringbone pattern (A). Gland-like structures formed by hyperplastic invaginated surface respiratory epithelium are frequently seen (B). Please see this image in color online.

rearrangement, or, as suggested by Dickson et al,<sup>19</sup> a relationship with the group of intracranial myxoid mesenchymal tumors with *EWSR1-CREB* family gene fusions.<sup>23,24</sup>

Biphenotypic sinonasal sarcoma (BSS) is a locally aggressive spindle cell neoplasm with distinctive histologic, immunohistochemical, and molecular features, mainly represented by *PAX3* gene rearrangements.<sup>25,26</sup> So far BSS has been reported only in the sinonasal tract, although an example of a spindle cell sarcoma with dual myogenic and neural phenotype and *RREB1-MKL2* chimeric transcription factor has been described in the oropharynx (see above).<sup>20</sup> Histologically, BSS presents as a subepithelial proliferation of bland, spindle cells with elongated and slender nuclei, arranged in fascicles with a herringbone pattern (Fig. 4). Typically, the tumor infiltrates the sinonasal mucosa and the bone, although necrosis is not seen, and mitotic activity is low. An accompanying epithelial proliferation, which consists of hyperplastic invaginated surface respiratory epithelium forming gland-like structures beneath the mucosal surface is frequently present. These epithelial elements are intimately associated with the neoplastic spindle cell component, imparting a biphasic pattern to the lesion, occasionally closely mimicking respiratory epithelial hamartomas, particularly in tumors with lower cellularity, or similar to biphasic synovial sarcoma. Other characteristic, but less frequent features include, branching dilated vessels and foci of hyaline collagen deposition. Focal rhabdomyoblastic differentiation, consisting of large strap-type cells with eosinophilic cytoplasm and focal cross-striations, has been observed.

The immunoprofile of BSS is complex, but the diagnosis requires combined immunoreactivity for S100 protein (focal to diffuse) and smooth muscle markers, mainly SMA, muscle specific actin, or calponin, whereas immunoreactivity for

desmin is only rarely seen and MYOD1 and myogenin are positive in cases showing areas of rhabdomyoblastic differentiation. Recently, immunohistochemical expression of *PAX3* was found to be highly sensitive and specific for the diagnosis of BSS.<sup>27</sup> Other positive markers include nuclear  $\beta$ -catenin and factor XIIIa,<sup>28,29</sup> while isolated keratin and epithelial membrane antigen (EMA) positive cells may also be seen. *SOX10* is consistently negative in the tumors tested.<sup>26</sup> Thus, the immunoprofile of BSS is complex and attention must be paid to the choice of the appropriate panel of markers in the differential diagnosis with other sinonasal spindle cell lesions. These include mainly *peripheral nerve sheath tumors*, which are also positive for *SOX10* and negative for muscle markers; *sinonasal glomangiopericytoma* that is positive for SMA and  $\beta$ -catenin, but negative for S100 protein; *solitary fibrous tumor*, which is positive for CD34 and STAT6, but negative for SMA and S100 protein; and *monophasic synovial sarcoma*, which may coexpress S100 protein and SMA, but is TLE1 and epithelial marker positive, with a different genetic profile.

Approximately 60% of tested BSS have a recurrent translocation t(2;4)(q35;q31.1) with a *PAX3-MAML3* fusion transcript that results in the activation of *PAX3* response elements. Alternative *PAX3* fusion partners include *FOXO1*, *NCOA1*, *NCOA2*, and *WWTR1*<sup>30-32</sup> with

*PAX3-NCOA1* in particular associated with the presence of rhabdomyoblastic differentiation.<sup>33</sup> A few cases have shown *PAX3* or *MAML3* rearrangements with unknown fusion partners or undetectable rearrangements.

### EPITHELIOD CELL TUMORS

Recently, a novel subset of mesenchymal tumors with *GLII* gene rearrangements or amplifications has been described.<sup>34–36</sup> These are rare but distinctive tumors with an established risk of malignancy that frequently occur in the head and neck, with a clear predilection for the tongue.<sup>36</sup> The fusion partner of *GLII* includes *ACTB* in the majority of the cases, whereas *MALAT1* and *PTCH1* are rarely identified partners. In tumors with *GLII* amplification, *MDM2* and *CDK4* are coamplified. These tumors occur over a wide age span, including infancy, with a median age in the fourth decade. At low power, they present a characteristic multinodular or plexiform growth pattern. Neoplastic cells are monomorphic, round to epithelioid, with clear or eosinophilic cytoplasm, and form nests separated by a delicate arborizing vascular network (Fig. 5). Typically, tumor nests tend to protrude into vascular spaces, an appearance reminiscent of pericytic growth (Fig. 5). Interestingly, soft tissue tumors with *ACTB-GLII* rearrangement had been previously reported as part of the spectrum of pericytomas.<sup>37,38</sup> The immunoprofile is variable, with frequent positivity for S100 protein and CD56.<sup>35,36</sup> SMA, AE1/AE3, and EMA are expressed in a minority of cases, while SOX10, CD31, CD34, ERG, chromogranin,

synaptophysin, CD99, and desmin are negative. *GLII*-amplified tumors are often positive for CDK4, MDM2, and STAT6 due to coamplification of these genes.

The main differential diagnosis is with salivary-type tumors, in particular with myoepithelioma and myoepithelial carcinoma,<sup>36</sup> that show some histologic overlap for the presence of epithelioid nested morphology, and S100 protein and cytokeratin positivity. However, tumors with *GLII* alterations have a rich vascular network separating the tumor nests, with tumor cells often bulging into vascular spaces, and are negative for SOX10, glial fibrillary acidic protein (GFAP), and calponin.<sup>36</sup> In addition, *GLII* molecular alterations have not been reported in salivary gland myoepithelial tumors. ECT may histologically resemble tumors with *GLII* alterations with its multilobulated architecture, and because of the positivity for cytokeratins, S100 protein, CD56, and SMA, but neoplastic cells are typically spindle shaped and set into abundant myxoid stroma without prominent capillary network, and they are often positive for calponin and GFAP. In addition, ECT has an *RREB1-MRTFB* fusion that can be tested for in difficult cases.<sup>19</sup> Finally, nested architecture and positivity for CD56 may elicit a diagnosis of neuroendocrine tumor, but other and more specific neuroendocrine markers (synaptophysin and chromogranin) are negative.<sup>34</sup>

### RHABDOMYOSARCOMA

RMS is the most frequent head and neck sarcoma both in adult and pediatric patients.<sup>4</sup> RMS classification has been

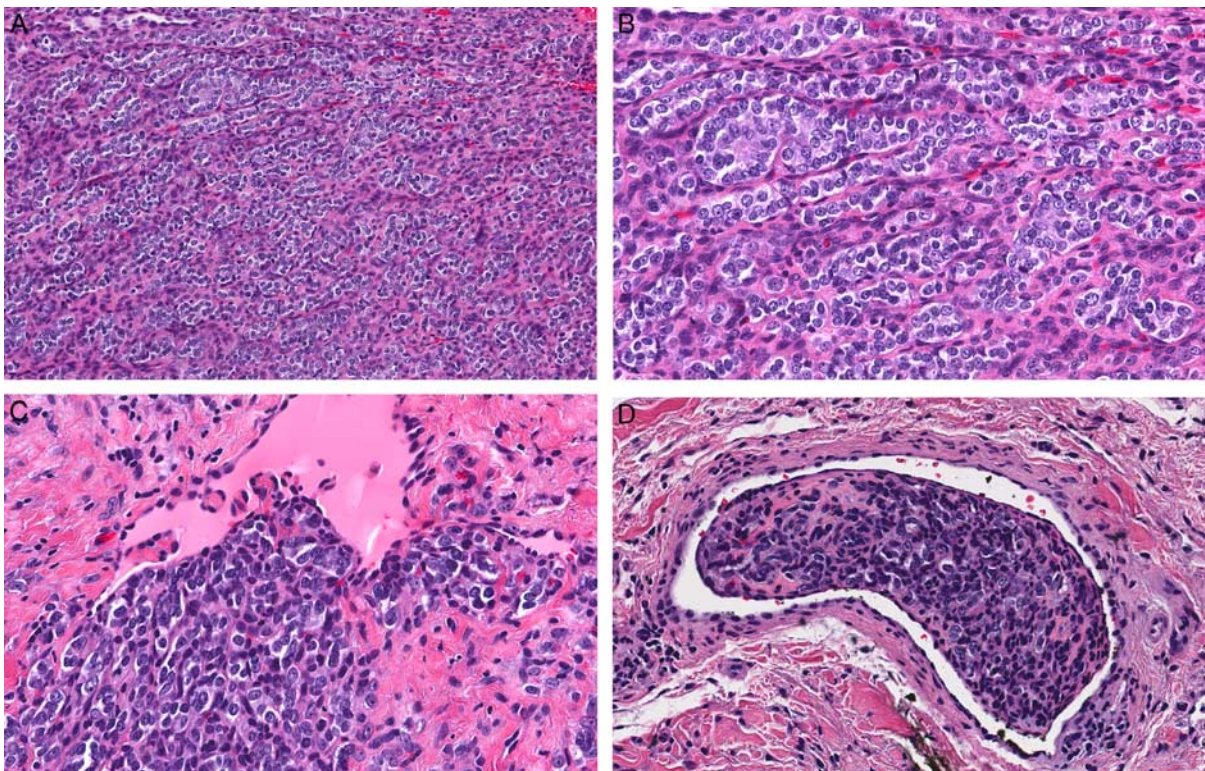


**FIGURE 5.** Mesenchymal tumor of the tongue with *GLII* gene rearrangement. This tumor presents solid nested architecture, with a delicate network of capillaries in the background (A). Neoplastic cells have a monotonous appearance, with round to ovoid nuclei and scant clear cytoplasm (B). Tumor nests are often associated with large vessels (C) and protrude into the ectatic lumen (D). Please see this image in color online.

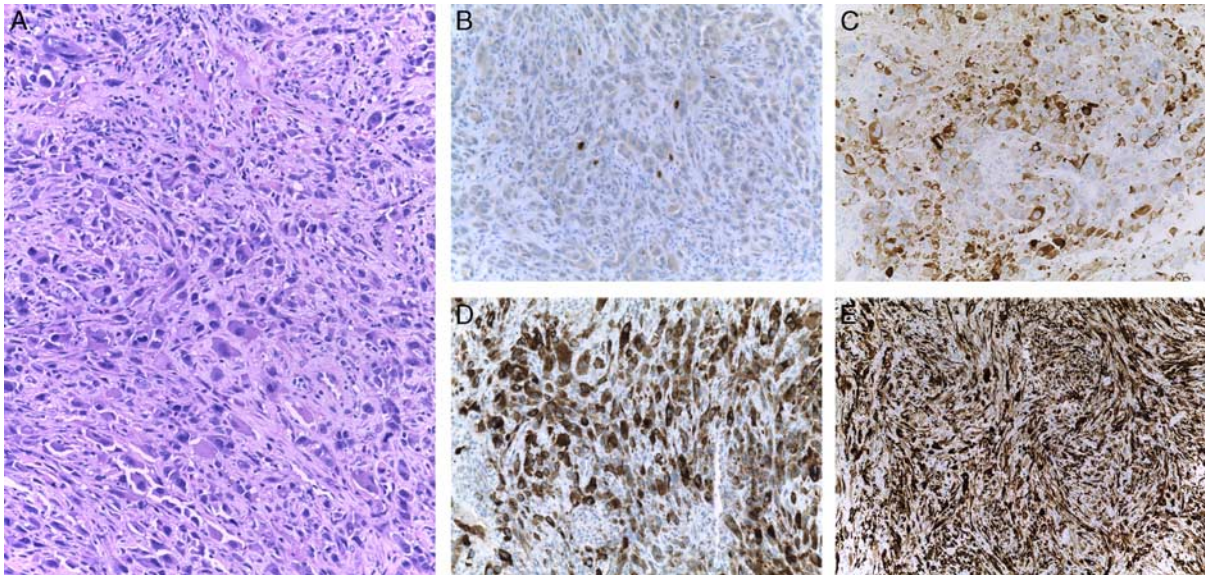


**FIGURE 6.** Epithelioid and spindle cell rhabdomyosarcoma with *EWSR1-TFCP2* fusion. This biopsy was taken from a lytic lesion of the mandible in a 32-year-old man. This highly pleomorphic tumor consists of spindle and epithelioid highly atypical cells (A), focally immunoreactive for MYF4 (B) and diffusely positive for desmin (C), ALK1 (D), and pancytokeratin (E). Please see this image in color online.

refined based on novel molecular findings, with the identification of new prognostic categories and of new histologic subtypes. The spindle cell/sclerosing RMS, which in adults occurs predominately in the head and neck region, now includes the *NCOA2*-rearranged RMS,<sup>39</sup> the *VGLL2*-rearranged RMS,<sup>40</sup> and spindle cell/sclerosing RMS with *MYOD1* mutations.<sup>41–45</sup>

This distinction is clinically relevant because among head and neck RMSs, spindle cell/sclerosing RMS with *MYOD1* mutation and alveolar RMS have a similar poor prognosis (5-y overall survival rate of 50% and 53%, respectively), compared with embryonal RMS (5-y overall survival rate of 82%).<sup>43,44,46</sup> Moreover, the *MYOD1*-mutant positive sclerosing RMS has a significantly worse prognosis than other spindle cell RMSs.<sup>46</sup> These studies strongly suggest that an *MYOD1* mutation is a marker of poor prognosis in RMS.

More recently, a new distinctive RMS variant with epithelioid and spindle cell morphology and *EWSR1/FUS-TFCP2* gene fusions has been identified. This RMS subtype has a striking predilection for involving craniofacial bones in young adults, associated with a very aggressive behavior, with patients dying after a median of 15 months despite multimodal therapy.<sup>47–49</sup> Histologically, these tumors are composed of variable proportions of spindle, epithelioid, and round cells that contain moderate to abundant eosinophilic cytoplasm, and oval nuclei with 1 or more prominent nucleoli (Fig. 6). Rare rhabdoid elements can be present. Abundant fibrous or myxoid stroma formation is only rarely seen. Mitotic activity is brisk, and necrosis is usually present. Among myogenic markers, desmin and *MYOD1* are diffusely positive, whereas myogenin is only focally expressed. Notably, epithelioid and spindle cell RMS is positive for pancytokeratin and ALK. S100 protein is focally positive in rare cases, whereas *SOX10* is negative. *ALK* RNA upregulation is present in the majority of the cases, whereas no rearrangement of the *ALK* gene has been detected.<sup>49</sup> Interestingly, the *ALK* gene is frequently deleted despite the presence of *ALK* overexpression. Other RMS subtypes, especially alveolar RMS, may show

*ALK* expression, but the significance of this finding is currently unknown.<sup>49</sup> The genetic hallmark of this RMS is the rearrangement of *TFCP2* gene with either *FUS* or *EWSR1*. Mutations of the *MYOD1* gene have not been identified.<sup>49</sup>

The differential diagnosis of epithelioid/spindle cell RMS includes other RMS subtypes such as purely epithelioid RMS, congenital/infantile spindle cell, and spindle cell/sclerosing RMS, although all these variants do not involve the bone. In contrast, the recently described intraosseous RMS with *MEIS-NCOA2* fusion presents with a fascicular proliferation of primitive spindle cells but has not been shown to involve craniofacial bones.<sup>47</sup> Because of the overlap of the immunohistochemical findings, including significant cytokeratin reactivity, sarcomatoid carcinoma must be included in the differential diagnosis of epithelioid/spindle cell RMS. Rhabdomyoblastic differentiation may also be present in sarcomatoid carcinoma, further complicating the issue. In difficult cases, testing for *TFCP2-EWS/FUS* rearrangements may be helpful. Other mesenchymal tumors that need to be distinguished from epithelioid/spindle RMS are leiomyosarcomas that do not express *MYOD1* and myogenin, and pseudomyogenic hemangioendothelioma, which may present some histologic overlap and shares positivity for cytokeratins, but it is characterized by more bland histologic features and positivity for ERG and FLI1.

## ROUND CELL SARCOMAS

Undifferentiated round cell neoplasms represent a diagnostic challenge in the head and neck region because they demonstrate overlapping morphologic and immunohistochemical features. A broad range of tumors may indeed present with undifferentiated round cell morphology, including the Ewing sarcoma (ES) family of tumors, synovial sarcoma, desmoplastic small round cell tumor, myxoid/round cell liposarcoma, small cell osteosarcoma, mesenchymal chondrosarcoma, and RMS, in addition to neuroectodermal tumors, melanoma, lymphoma, and carcinomas.

ES is the prototypical round cell sarcoma characterized by specific gene fusions involving the *EWSRI* gene and member of the ETS transcription factor family (*FLII*, *ERG*, *ETV1*, *ETV4*, or *FEV*). Recent approaches have focused on round cell sarcomas that lack the specific translocations of ES, using new genomic techniques to identify new translocation-specific sarcomas. This emerging group of Ewing-like sarcomas include round cell sarcomas with *EWSRI* gene fusion with non-ETS gene family members (such as *NFATc2*), *CIC*-rearranged sarcomas (CRSs), and *BCOR*-rearranged sarcomas.<sup>50</sup>

Besides classic ES, the head and neck region is the site of an intriguing ES variant, the adamantinoma-like ES. Although this tumor type was first described in 1999 in long bones,<sup>51</sup> it has recently emerged as a tumor predominantly involving the head and neck with a wide anatomic distribution, including mucosal sites and glands (parotid and thyroid).<sup>52</sup> Histologically, it consists of sheets or nests of round cells with basaloid appearance within fibrous, myxoid, or hyalinized matrix (Fig. 7). Nuclear palisading and rosette formation can be present. Foci of squamous differentiation, with formation of keratin pearls are seen in a minority of cases. Mitotic activity is brisk and foci of necrosis are often present. Immunohistochemical studies show diffuse expression of

ES markers including CD99, FLI1, and NKX2.2 (Fig. 7), and positivity for cytokeratins (including cytokeratin 5/6), p63 and p40 (Table 2). Neuroendocrine markers are often positive as well.<sup>52</sup> S100 protein, SMA, desmin, WT1, and NUT1 are negative.<sup>52</sup> At the molecular level adamantinoma-like ES presents the typical t(11;22) *EWSRI-FLII* translocation of ES (Table 2). Given the extensive morphologic and immunohistochemical overlap with several other head and neck malignancies, molecular confirmation is often performed to support the diagnosis. An *EWSRI* break-apart FISH test alone may not be sufficient to exclude a myoepithelial tumor, thus either reverse transcription-polymerase chain reaction for *EWSRI-FLII* fusion or FISH analysis for *FLII* gene rearrangement can be used to confirm the diagnosis of adamantinoma-like ES. Besides myoepithelial tumors, adamantinoma-like ES must be distinguished from several other head and neck tumor types that can present with a poorly differentiated/basaloid morphology, including adamantinoma, synovial sarcoma, NUT carcinoma, basaloid squamous cell carcinoma, neuroendocrine carcinoma, *SMARCB1*-deficient carcinoma, desmoplastic small round cell tumor, basal cell adenocarcinoma, poorly differentiated thyroid carcinoma, medullary thyroid carcinoma, and carcinoma showing thymus-like differentiation (CASTLE).<sup>52-56</sup>

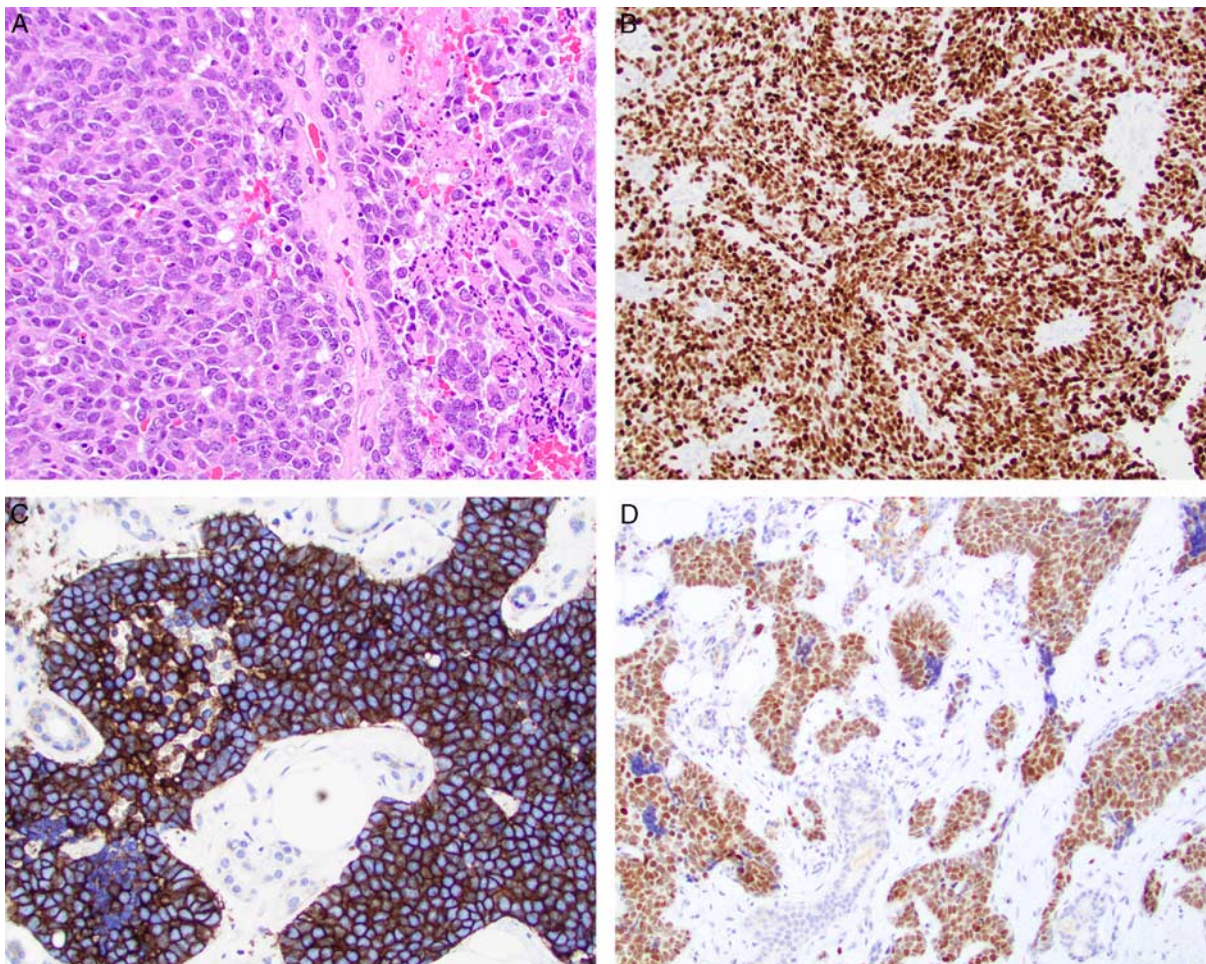


**FIGURE 7.** At high power, there is a basaloid, primitive-appearing neoplastic proliferation with areas of central necrosis in this adamantinoma-like Ewing sarcoma (A). The neoplastic cells show a strong and diffuse nuclear reaction with p40 (B), whereas CD99 (C) and NKX2.2 (D) are also strongly reactive. Please see this image in color online.

TABLE 2. Diagnostic Markers of Emerging Head and Neck Round Cell Sarcomas

Tumor Type	CD99	FLI1	NKX2.2	WT1	ETV4	DUX4	BCOR	Cy. D1	SATB2	Cy. D3	CK	p63	p40	Gene Fusion(s)
Adamaninoma-like EWS	+	+	+	-	+	-	-	+, tested in conventional ES	-*	-	+	+	+	<i>EWSR1-FLI1</i>
<i>CIC</i> -rearranged sarcoma	+, not diffuse	+	+	+	+	+	-	NT	NT	-	+, rare	-	-	<i>CIC-DUX4</i> (95%) <i>CIC-FOXO4</i> <i>CIC-LEUTX</i> <i>CIC-NUTM1</i> <i>CIC-NUTM2</i>
Sarcoma with <i>BCOR</i> genetic alterations	+, not diffuse	NT	+	NT	-	NT	+	+	+	+†	-	+	-	<i>BCOR-CCNB3</i> <i>BCOR-MAML2</i> <i>BCOR-ITD</i>

\*Focal weak staining in rare cases of conventional EWS tested.

†In tumors with *CCND3* rearrangement.

+ indicates positive staining; -, negative staining; CK, cytokeratin; Cy, cyclin; EWS, Ewing sarcoma; ITD, internal tandem duplication; NT, not tested.

CRS predominately occurs in children and young adults, presents an aggressive clinical behavior, and very rarely occurs in the head and neck. Owosho et al<sup>57</sup> studied a group of 16 CRSs arising in the head and neck and compared their clinicopathologic features with those of a group of 25 ESs. CRSs exclusively involved the soft tissues, with the neck being the most common location, and the median age at diagnosis was 28.5 years.<sup>57</sup> Histologically, tumors present with a solid growth pattern, often with a nodular architecture. The neoplastic population is less homogeneous than in ES, being composed of primitive round to ovoid cells often intermixed with areas of spindle and epithelioid cells with a more abundant cytoplasm (Fig. 8). Mitotic activity is brisk and geographic necrosis is often seen. Positive immunostains include CD99 (often focal and/or weak staining), WT1, DUX4, ETV4, and occasional cases may show focal expression of cytokeratins, EMA, ERG, S100 protein, and desmin<sup>58-61</sup> (Table 2). Chromogranin, synaptophysin, and lymphoid markers are negative. The *CIC-DUX4* gene fusion results from either a t(4;19) or t(10;19) translocation, whereas rare cases may present non-*DUX4* partners such as *FOXO4*, *LEUTX*, *NUTM1*, and *NUTM2*.<sup>62-64</sup> The chimeric gene includes most of the coding sequence of *CIC* and a small portion of the 3' end of *DUX4*. Although it has been emphasized that CRS is a highly aggressive tumor with poor response to ES treatment regimens, no significant differences were found in overall survival between CRS and ES arising in the head and neck.<sup>57</sup>

An additional group of *EWSR1*-negative undifferentiated round cell sarcomas presents a recurrent *BCOR-CCNB3* rearrangement. These tumors have a predilection for skeletal sites and are exceptionally rare in the head and neck. In the series studied by Kao et al<sup>65</sup> one tumor arising in a 13-year-old female patient was located in the soft palate and one arising in a 2-year-old male patient was located in the posterior neck. A further example involving the skull base in a 5-year-old boy was reported by Specht et al.<sup>66</sup> Histologically, *BCOR-CCNB3* sarcoma is composed of a uniform population of fusiform to ovoid cells arranged in sheets or short fascicles, often accompanied by a delicate capillary network (Fig. 9). Myxoid stroma may be present in some instances. Immunohistochemical positivity for cyclin B3, the product of *CCNB3* gene, is a useful marker to confirm the diagnosis,<sup>66-68</sup> whereas *BCOR* is less specific. Other positive markers include SATB2, TLE1, cyclin D1, and EMA

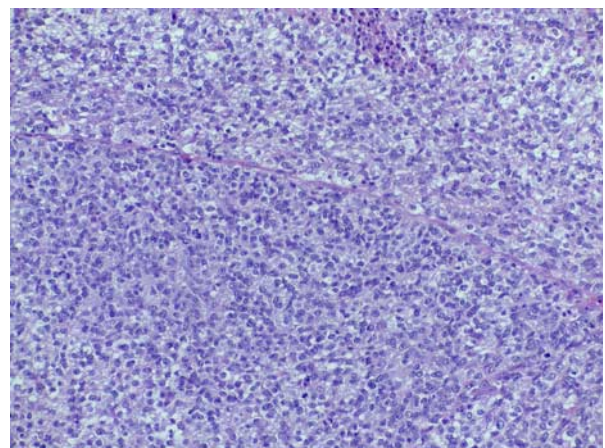
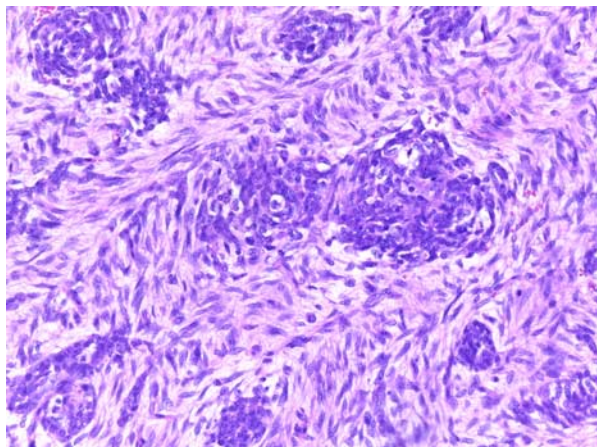


FIGURE 8. Undifferentiated round cell sarcoma with *CIC-DUX4* fusion. The neoplastic population shows minimal degree of pleomorphism. Please see this image in color online.





**FIGURE 9.** *BCOR-CCNB3* fusion positive sarcoma. Neoplastic cells with primitive morphology are arranged within myxoid stroma and form clusters. This tumor presented an inv(X)(p11p11) *BCOR-CCNB3* rearrangement. Please see this image in color online.

(weak positivity)<sup>69–71</sup> (Table 2). This possibility should be kept in mind in the differential diagnosis with small cell osteosarcoma and synovial sarcoma. Molecular confirmation of *BCOR* rearrangement is particularly useful in these cases.

Besides the *BCOR-CCNB3* sarcoma, sarcomas with *BCOR*-variant fusions with a non-*CCNB3* partner, and sarcomas with internal tandem duplications of *BCOR* exon 15 have been recognized. Immunohistochemistry against *BCOR* and *CCNB3* is helpful in screening for these rare tumors. A tumor arising in the sinonasal tract in a 48-year-old woman presented with the *CIITA-BCOR* fusion.<sup>72</sup> Histologically, this tumor consisted of a uniform population of spindle/ovoid cells set in variable amounts of myxoid stroma. Immunohistochemically, it was positive for *BCOR*, *SATB2*, and *CD99*, whereas *INI1* and *H3K27me3* were retained. Cytokeratins *AE1/AE3*, *EMA*, *S100* protein, *SMA*, *desmin*, *STAT6*, *CD34*, *synaptophysin*, *chromogranin A*, *c-kit*, *HMB45*, *GFAP*, *NKX2.2*, *MUC4*, and *CCNB3* were negative.<sup>71</sup> The tumor was surgically treated and recurred 3 times locally.<sup>71</sup> Interestingly, the *BCOR* family of tumors commonly shows *NTRK3* upregulation resulting in pan-Trk immunohistochemical overexpression, but the therapeutic implications of these findings are still to be elucidated.<sup>73</sup>

## REFERENCES

- Potter BO, Sturgis EM. Sarcomas of the head and neck. *Surg Oncol Clin N Am*. 2003;12:379–417.
- Daw NC, Mahmoud HH, Meyer WH, et al. Bone sarcomas of the head and neck in children: the St Jude Children's Research Hospital experience. *Cancer*. 2000;88:2172–2180.
- Vassiliou LV, Lalabekyan B, Jay A, et al. Head and neck sarcomas: a single institute series. *Oral Oncol*. 2017;65:16–22.
- Kalavrezos N, Sinha D. Head and neck sarcomas in adulthood: current trends and evolving management concepts. *Br J Oral Maxillofac Surg*. 2020;58:890–897.
- Kanagal-Shamanna R, Portier BP, Singh RR, et al. Next-generation sequencing-based multi-gene mutation profiling of solid tumors using fine needle aspiration samples: promises and challenges for routine clinical diagnostics. *Mod Pathol*. 2014;27:314–327.
- Zhu H, Sun J, Wei S, et al. Well-differentiated laryngeal/hypopharyngeal liposarcoma in the MDM2 era report of three cases and literature review. *Head Neck Pathol*. 2017;11:146–151.
- Fritchie K, Ghosh T, Graham RP, et al. Well-differentiated/dedifferentiated liposarcoma arising in the upper aerodigestive tract: 8 cases mimicking non-adipocytic lesions. *Head Neck Pathol*. 2020;14:974–981.
- Waters R, Horvai A, Greipp P, et al. Atypical lipomatous tumour/well-differentiated liposarcoma and de-differentiated liposarcoma in patients aged  $\leq 40$  years: a study of 116 patients. *Histopathology*. 2019;75:833–842.
- Sbaraglia M, Dei Tos AP, Pedeutour F. Atypical lipomatous tumor/well differentiated liposarcoma. In: WHO Classification of Tumors Editorial Board, ed. *Soft Tissue and Bone Tumours*. Lyon, France: IARC; 2020.
- Stojanov IJ, Mariño-Enríquez A, Bahri N, et al. Lipomas of the oral cavity: utility of MDM2 and CDK4 in avoiding over-diagnosis as atypical lipomatous tumor. *Head Neck Pathol*. 2019;13:169–176.
- Doyle LA, Vivero M, Fletcher CD, et al. Nuclear expression of STAT6 distinguishes solitary fibrous tumor from histologic mimics. *Mod Pathol*. 2014;27:390–395.
- Doyle LA, Tao D, Mariño-Enríquez A. STAT6 is amplified in a subset of dedifferentiated liposarcoma. *Mod Pathol*. 2014;27:1231–1237.
- Cretyens D, Marino-Enriquez A. Atypical spindle cell/pleomorphic lipomatous tumor. In: WHO Classification of Tumors Editorial Board, ed. *Soft Tissue and Bone Tumours*. Lyon, France: IARC; 2020:34–35.
- Mariño-Enríquez A, Nascimento AF, Ligon AH, et al. Atypical spindle cell lipomatous tumor: clinicopathologic characterization of 232 cases demonstrating a morphologic spectrum. *Am J Surg Pathol*. 2017;41:234–244.
- Cretyens D, Mentzel T, Ferdinande L, et al. “Atypical” pleomorphic lipomatous tumor: a clinicopathologic, immunohistochemical and molecular study of 21 cases, emphasizing its relationship to atypical spindle cell lipomatous tumor and suggesting a morphologic spectrum (atypical spindle cell/pleomorphic lipomatous tumor). *Am J Surg Pathol*. 2017;41:1443–1455.
- Chen BJ, Mariño-Enríquez A, Fletcher CD, et al. Loss of retinoblastoma protein expression in spindle cell/pleomorphic lipomas and cytogenetically related tumors: an immunohistochemical study with diagnostic implications. *Am J Surg Pathol*. 2012;36:1119–1128.
- Smith BC, Ellis GL, Meis-Kindblom JM, et al. Ectomesenchymal chondromyxoid tumor of the anterior tongue. Nineteen cases of a new clinicopathologic entity. *Am J Surg Pathol*. 1995;19:519–530.
- Bubola J, Hagen K, Blanas N, et al. Expanding awareness of the distribution and biologic potential of ectomesenchymal chondromyxoid tumor. *Head Neck Pathol*. 2020. [Epub ahead of print].
- Dickson BC, Antonescu CR, Argyris PP, et al. Ectomesenchymal chondromyxoid tumor: a neoplasm characterized by recurrent *RREB1-MKL2* fusions. *Am J Surg Pathol*. 2018;42:1297–1305.
- Siegfried A, Romary C, Escudie F, et al. *RREB1-MKL2* fusion in biphenotypic ‘oropharyngeal’ sarcoma: new entity or part of the spectrum of biphenotypic sinonasal sarcomas? *Genes Chromosomes Cancer*. 2018;57:203–210.
- Makise N, Mori T, Kobayashi H, et al. Mesenchymal tumours with *RREB1-MRTFB* fusion involving the mediastinum: extraglossal ectomesenchymal chondromyxoid tumours? *Histopathology*. 2020;76:1023–1031.
- Argyris PP, Bilodeau EA, Yancoskie AE, et al. A subset of ectomesenchymal chondromyxoid tumours of the tongue show *EWSR1* rearrangements and are genetically linked to soft tissue myoepithelial neoplasms: a study of 11 cases. *Histopathology*. 2016;69:607–613.
- Kao YC, Sung YS, Zhang L, et al. *EWSR1* fusions with *CREB* family transcription factors define a novel myxoid mesenchymal tumor with predilection for intracranial location. *Am J Surg Pathol*. 2017;41:482–490.
- Velz J, Agaimy A, Frontzek K, et al. Molecular and clinicopathologic heterogeneity of intracranial tumors mimicking extraskeletal myxoid chondrosarcoma. *J Neuropathol Exp Neurol*. 2018;77:727–735.

25. Fritchie KJ, Jin L, Wang X, et al. Fusion gene profile of biphenotypic sinonasal sarcoma: an analysis of 44 cases. *Histopathology*. 2016;69:930–936.
26. Andreasen S, Bishop JA, Hellquist H, et al. Biphenotypic sinonasal sarcoma: demographics, clinicopathological characteristics, molecular features, and prognosis of a recently described entity. *Virchows Arch*. 2018;473:615–626.
27. Jo VY, Mariño-Enríquez A, Fletcher CDM, et al. Expression of PAX3 distinguishes biphenotypic sinonasal sarcoma from histologic mimics. *Am J Surg Pathol*. 2018;42:1275–1285.
28. Rooper LM, Huang SC, Antonescu CR, et al. Biphenotypic sinonasal sarcoma: an expanded immunoprofile including consistent nuclear  $\beta$ -catenin positivity and absence of SOX10 expression. *Hum Pathol*. 2016;55:44–50.
29. Kakkar A, Rajeshwari M, Sakthivel P, et al. Biphenotypic sinonasal sarcoma: a series of six cases with evaluation of role of  $\beta$ -catenin immunohistochemistry in differential diagnosis. *Ann Diagn Pathol*. 2018;33:6–10.
30. Wang X, Bledsoe KL, Graham RP, et al. Recurrent PAX3-MAML3 fusion in biphenotypic sinonasal sarcoma. *Nat Genet*. 2014;46:666–668.
31. Wong WJ, Lauria A, Hornick JL, et al. Alternate PAX3-FOXO1 oncogenic fusion in biphenotypic sinonasal sarcoma. *Genes Chromosomes Cancer*. 2016;55:25–29.
32. Le Loarer F, Laffont S, Lesluyes T, et al. Clinicopathologic and molecular features of a series of 41 biphenotypic sinonasal sarcomas expanding their molecular spectrum. *Am J Surg Pathol*. 2019;43:747–754.
33. Huang SC, Ghossein RA, Bishop JA, et al. Novel PAX3-NCOA1 fusions in biphenotypic sinonasal sarcoma with focal rhabdomyoblastic differentiation. *Am J Surg Pathol*. 2016;40:51–59.
34. Antonescu CR, Agaram NP, Sung YS, et al. A distinct malignant epithelioid neoplasm with GLI1 gene rearrangements, frequent s100 protein expression, and metastatic potential: expanding the spectrum of pathologic entities with ACTB/MALAT1/PTCH1-GLI1 fusions. *Am J Surg Pathol*. 2018;42:553–560.
35. Agaram NP, Zhang L, Sung YS, et al. GLI1-amplifications expand the spectrum of soft tissue neoplasms defined by GLI1 gene fusions. *Mod Pathol*. 2019;32:1617–1626.
36. Xu B, Chang K, Folpe AL, et al. Head and neck mesenchymal neoplasms with GLI1 gene alterations: a pathologic entity with distinct histologic features and potential for distant metastasis. *Am J Surg Pathol*. 2020;44:729–737.
37. Bridge JA, Sanders K, Huang D, et al. Pericytoma with t(7;12) and ACTB-GLI1 fusion arising in bone. *Hum Pathol*. 2012;43:1524–1529.
38. Dahlen A, Fletcher CD, Mertens F, et al. Activation of the GLI oncogene through fusion with the beta-actin gene (ACTB) in a group of distinctive pericytic neoplasms: pericytoma with t(7;12). *Am J Pathol*. 2004;164:1645–1653.
39. Mosquera JM, Sboner A, Zhang L, et al. Recurrent NCOA2 gene rearrangements in congenital/infantile spindle cell rhabdomyosarcoma. *Genes Chromosomes Cancer*. 2013;52:538–550.
40. Alaggio R, Zhang L, Sung YS, et al. A molecular study of pediatric spindle and sclerosing rhabdomyosarcoma: identification of novel and recurrent VGLL2-related fusions in infantile cases. *Am J Surg Pathol*. 2016;40:224–235.
41. Kohsaka S, Shukla N, Ameer N, et al. A recurrent neomorphic mutation in MYOD1 defines a clinically aggressive subset of embryonal rhabdomyosarcoma associated with PI3K-AKT pathway mutations. *Nat Genet*. 2014;46:595–600.
42. Szuhai K, de Jong D, Leung WY, et al. Transactivating mutation of the MYOD1 gene is a frequent event in adult spindle cell rhabdomyosarcoma. *J Pathol*. 2014;232:300–307.
43. Agaram NP, LaQuaglia MP, Alaggio R, et al. MYOD1-mutant spindle cell and sclerosing rhabdomyosarcoma: an aggressive subtype irrespective of age. A reappraisal for molecular classification and risk stratification. *Mod Pathol*. 2019;32:27–36.
44. Rekhi B, Upadhyay P, Ramteke MP, et al. MYOD1 (L122R) mutations are associated with spindle cell and sclerosing rhabdomyosarcomas with aggressive clinical outcomes. *Mod Pathol*. 2016;29:1532–1540.
45. Tsai JW, ChangChien YC, Lee JC, et al. The expanding morphological and genetic spectrum of MYOD1-mutant spindle cell/sclerosing rhabdomyosarcomas: a clinicopathological and molecular comparison of mutated and nonmutated cases. *Histopathology*. 2019;74:933–943.
46. Owosho AA, Huang SC, Chen S, et al. A clinicopathologic study of head and neck rhabdomyosarcomas showing FOXO1 fusion-positive alveolar and MYOD1-mutant sclerosing are associated with unfavorable outcome. *Oral Oncol*. 2016;61:89–97.
47. Agaram NP, Zhang L, Sung YS, et al. Expanding the spectrum of intraosseous rhabdomyosarcoma: correlation between 2 distinct gene fusions and phenotype. *Am J Surg Pathol*. 2019;43:695–702.
48. Chrisinger JSA, Wehrli B, Dickson BC, et al. Epithelioid and spindle cell rhabdomyosarcoma with FUS-TFCP2 or EWSR1-TFCP2 fusion: report of two cases. *Virchows Arch*. 2020;477:725–732.
49. Le Loarer F, Cleven AHG, Bouvier C, et al. A subset of epithelioid and spindle cell rhabdomyosarcomas is associated with TFCP2 fusions and common ALK upregulation. *Mod Pathol*. 2020;33:404–419.
50. Bridge JA, ed. WHO Classification of Tumors Editorial Board. Undifferentiated small round cell sarcomas of bone and soft tissues. *Soft Tissue and Bone Tumours*. Lyon, France: IARC; 2020.
51. Bridge JA, Fidler ME, Neff JR, et al. Adamantinoma-like Ewing's sarcoma: genomic confirmation, phenotypic drift. *Am J Surg Pathol*. 1999;23:159–165.
52. Rooper LM, Bishop JA. Soft tissue special issue: adamantinoma-like Ewing sarcoma of the head and neck: a practical review of a challenging emerging entity. *Head Neck Pathol*. 2020;14:59–69.
53. Rooper LM, Jo VY, Antonescu CR, et al. Adamantinoma-like Ewing sarcoma of the salivary glands: a newly recognized mimicker of basaloid salivary carcinomas. *Am J Surg Pathol*. 2019;43:187–194.
54. Bishop JA, Alaggio R, Zhang L, et al. Adamantinoma-like Ewing family tumors of the head and neck: a pitfall in the differential diagnosis of basaloid and myoepithelial carcinomas. *Am J Surg Pathol*. 2015;39:1267–1274.
55. Alexiev BA, Tumer Y, Bishop JA. Sinonasal adamantinoma-like Ewing sarcoma: a case report. *Pathol Res Pract*. 2017;213:422–426.
56. Lilo MT, Bishop JA, Olson MT, et al. Adamantinoma-like Ewing sarcoma of the parotid gland: cytopathologic findings and differential diagnosis. *Diagn Cytopathol*. 2018;46:263–266.
57. Owosho AA, Estilo CL, Hury JM, et al. Head and neck round cell sarcomas: a comparative clinicopathologic analysis of 2 molecular subsets: Ewing and CIC-rearranged sarcomas. *Head Neck Pathol*. 2017;1:450–459.
58. Hung YP, Fletcher CD, Hornick JL. Evaluation of ETV4 and WT1 expression in CIC-rearranged sarcomas and histologic mimics. *Mod Pathol*. 2016;29:1324–1334.
59. Le Guellec S, Velasco V, Pérot G, et al. ETV4 is a useful marker for the diagnosis of CIC-rearranged undifferentiated round cell sarcomas: a study of 127 cases including mimicking lesions. *Mod Pathol*. 2016;29:1523–1531.
60. Siegele B, Roberts J, Black JO, et al. DUX4 immunohistochemistry is a highly sensitive and specific marker for CIC-DUX4 fusion-positive round cell tumor. *Am J Surg Pathol*. 2017;41:423–429.
61. Sbaraglia M, Righi A, Gambarotti M, et al. Ewing sarcoma and Ewing-like tumors. *Virchows Arch*. 2020;476:109–119.
62. Sugita S, Arai Y, Tonooka A, et al. A novel CIC-FOXO4 gene fusion in undifferentiated small round cell sarcoma: a genetically distinct variant of Ewing-like sarcoma. *Am J Surg Pathol*. 2014;38:1571–1576.
63. Sugita S, Arai Y, Aoyama T, et al. NUTM2A-CIC fusion small round cell sarcoma: a genetically distinct variant of CIC-rearranged sarcoma. *Hum Pathol*. 2017;65:225–230.
64. Le Loarer F, Pissaloux D, Watson S, et al. Clinicopathologic features of CIC-NUTM1 sarcomas, a new molecular variant of the family of CIC-fused sarcomas. *Am J Surg Pathol*. 2019;43:268–276.

65. Kao YC, Owosho AA, Sung YS, et al. BCOR-CCNB3 fusion positive sarcomas: a clinicopathologic and molecular analysis of 36 cases with comparison to morphologic spectrum and clinical behavior of other round cell sarcomas. *Am J Surg Pathol*. 2018;42:604–615.
66. Specht K, Zhang L, Sung YS, et al. Novel BCOR-MAML3 and ZC3H7B-BCOR gene fusions in undifferentiated small blue round cell sarcomas. *Am J Surg Pathol*. 2016;40:433–442.
67. Shibayama T, Okamoto T, Nakashima Y, et al. Screening of BCOR-CCNB3 sarcoma using immunohistochemistry for CCNB3: a clinicopathological report of three pediatric cases. *Pathol Int*. 2015;65:410–414.
68. Kao YC, Sung YS, Zhang L, et al. BCOR overexpression is a highly sensitive marker in round cell sarcomas with BCOR genetic abnormalities. *Am J Surg Pathol*. 2016;40:1670–1678.
69. Matsuyama A, Shiba E, Umekita Y, et al. Clinicopathologic diversity of undifferentiated sarcoma with BCOR-CCNB3 fusion: analysis of 11 cases with a reappraisal of the utility of immunohistochemistry for BCOR and CCNB3. *Am J Surg Pathol*. 2017;41:1713–1721.
70. Yamada Y, Kuda M, Kohashi K, et al. Histological and immunohistochemical characteristics of undifferentiated small round cell sarcomas associated with CIC-DUX4 and BCOR-CCNB3 fusion genes. *Virchows Arch*. 2017;470:373–380.
71. Creytens D. SATB2 and TLE1 expression in BCOR-CCNB3 (Ewing-like) sarcoma, mimicking small cell osteosarcoma and poorly differentiated synovial sarcoma. *Appl Immunohistochem Mol Morphol*. 2020;28:e10–e12.
72. Yoshida A, Arai Y, Hama N, et al. Expanding the clinicopathologic and molecular spectrum of BCOR-associated sarcomas in adults. *Histopathology*. 2020;76:509–520.
73. Kao YC, Sung YS, Argani P, et al. NTRK3 overexpression in undifferentiated sarcomas with YWHAE and BCOR genetic alterations. *Mod Pathol*. 2020;33:1341–1349.